Journal of Engineering Mathematics **41:** 189–201, 2001.

Numerical 2D models of consolidation of dense flocculated suspensions

KATARINA GUSTAVSSON and JESPER OPPELSTRUP
Department of Numerical Analysis and Computing Science, Royal Institute of Technology, S-100 44 Stockholm, Sweden

Received 26 June 2000; accepted in revised form 2 May 2001

Abstract. A mathematical 2D model for a consolidation process of a highly concentrated, flocculated suspension is developed. The suspension is treated as a mixture of a fluid and solid particles by an Eulerian two-phase fluid model. The suspension is characterized by constitutive relations correlating the stresses, interaction forces, and inter-particle forces to concentration and velocity gradients. This results in three empirical material functions: a permeability, a non-Newtonian viscosity and a non-reversible particle interaction pressure. Parameters in the models are fitted to experimental data. A simulation program using finite difference methods both in time and space is applied to one and two dimensional test cases. The effect of different viscosity models as well as the effect of shear on consolidation rate is studied. The results show that a shear thinning viscosity model yields a higher consolidation rate compared to a model that only depends on the volume fraction. It is also concluded that the size of the viscosity influences the time scale of the process and that the expected effect of shear on the process is not weil reproduced with any of the models.

Key words: consolidation, flocculated suspension, Eulerian two-fluid model, shear thinning, numerical simulations.

1. Introduction

Sedimentation and consolidation are separation techniques used in many industrial applications such as dewatering of paper pulp, industrial waste water and mineral tailings.

In this paper we present a mathematical model and a numerical 2D study of a gravity induced consolidation process of a dense flocculated suspension. The suspension we consider is a binary mixture of water and large agglomerates of particles, flocs. The idea is to simulate a separation process of industrial waste water.

The flow of a fluid with dispersed particles or flocs can be modeled in different ways depending on the application as well as the number of of particles in the fluid. Recent approaches are direct simulations, see *e.g.*, Glowinski *et al.* [1] and Maury [2]. This is, however, only feasible for a limited number of particles. Since we are interested in a concentrated, flocculated suspension where the number of particles is large, we consider the problem from a macroscopical point of view.

The suspension is modeled as a two-constituent fluid-particle mixture, where the two phases are treated as interpenetrating continua. We refer to this model as the Eulerian two-fluid model and this type of model is discussed in Drew and Passman [3] and Bustos *et al.* [4, Chapter 3] among others. This is a rather general model and it has been used in different applications such as dewatering of paper pulp, Zahrai [5] and fluidized beds, Enwald *et al.*

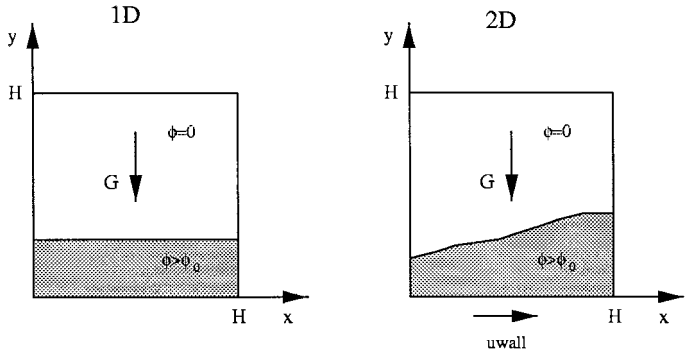

Figure 1. Schematic picture of the consolidation process. Closed container with a moving or fixed bottom wall. Gravity pointing in negative y-direction

[6]. This model is also the starting point for many of the classical 1D consolidation problems, treated in *e.g.*, Auzerais *et al.* [7], Bürger and Concha [8] and in Dorobantu [9].

In the simulation the suspension is confined to a closed box. Under the influence of gravity and shear, accomplished by a continuous movement of the bottom wall, the suspension is irreversibly compressed and the solid phase is separated from the liquid phase. The process is shown in Figure 1.

The first part of this paper treats the mathematical model. To make the two-fluid model complete, one must add constitutive models for the stress-strain relations and the interaction between the phases. We relate these models to three empirical material functions: a permeability, a non-Newtonian viscosity and a non-reversible particle interaction pressure. This is discussed in the second part of this paper. We also discuss the determination of different parameter values for the constitutive models by fitting to experimental data. In the third part, a simulation program is described and results of numerical experiments on au industrial application are presented. Specifically, the effects of different viscosity models are investigated.

2. Mathematical formulation

2.1. Eulerian two-fluid model

The Eulerian two-fluid model is based on a macroscopic description of the process. The two phases are treated as separate interpenetrating continua and mean equations are formulated for conservation of mass and momentum. The phases are coupled through inter-phase momentum transfer terms. This model is discussed in detail in Passman and Drew [3, pp. 137–231].

If surface tension effects are neglected and there is no mass transfer between the phases, the conservation of mass and momentum for each phase can be formulated as follows

$$\phi_t + \nabla \cdot (\phi \boldsymbol{u}) = 0, \tag{1}$$

$$\nabla \cdot (\phi \boldsymbol{u} + (1-\phi)\boldsymbol{v}) = 0, \tag{2}$$

$$\rho_s \phi \frac{\mathrm{D}\boldsymbol{u}}{\mathrm{D}t} + \phi \nabla p_f - \nabla \cdot \boldsymbol{T}_s = \rho_s \phi \boldsymbol{g} + \boldsymbol{m}, \tag{3}$$

$$\rho_f (1-\phi) \frac{\mathrm{D}\boldsymbol{v}}{\mathrm{D}t} + (1-\phi)\nabla p_f - \nabla \cdot \boldsymbol{\tau}_f = \rho_f (1-\phi)\boldsymbol{g} - \boldsymbol{m}, \tag{4}$$

$$\frac{\mathrm{D}\boldsymbol{u}}{\mathrm{D}t} = (\boldsymbol{u}_t + \boldsymbol{u}\cdot\nabla\boldsymbol{u})\ \frac{\mathrm{D}\boldsymbol{v}}{\mathrm{D}t} = (\boldsymbol{v}_t + \boldsymbol{v}\cdot\nabla\boldsymbol{v}).$$

Subscript s denotes the solid phase and f denotes the fluid phase. The volume fraction of solids is denoted by $\phi \in [0, 1]$, ρ is the density and $\boldsymbol{u}, \boldsymbol{v} \in \mathbb{R}^2$ are the velocities of the solid and fluid phase respectively. The fluid pressure is denoted by $p_f \in \mathbb{R}^+$. The solids stress tensor $\boldsymbol{T} \in \mathbb{R}^{2\times2}$ and the fluid viscous stress tensor $\boldsymbol{\tau} \in \mathbb{R}^{2\times2}$ will be discussed below together with the inter-phase momentum transfer term $\boldsymbol{m} \in \mathbb{R}^2$.

3. Constitutive relations

Constitutive laws are necessary to form a closed set of equations and to accomplish the characterization of the material. In this section the models are discussed from a general point of view and Section 6 gives more details and explains determination of the parameters from experimental data.

3.1. Stresses

The solid phase is assumed to support shear forces only when velocity gradients are present, i.e., in this respect to behave like a fluid, with stress tensor

$$T_s = -p_s\boldsymbol{I} + \boldsymbol{\tau}_s, \tag{5}$$

where

$$\boldsymbol{\tau}_s = \eta_s(\nabla\boldsymbol{u} + \nabla\boldsymbol{u}^T) - \tfrac{2}{3}\eta_s(\nabla\cdot\boldsymbol{u})\boldsymbol{I},$$

with η_s the viscosity of the particle phase. In the material studied the viscosity of the mixture is dominated by the particle phase viscosity except in the clear fluid limit. We will therefore assume that the mixture viscosity $\eta_{\mathrm{mix}} = \eta_s$. Furthermore, we assume that the mixture viscosity is a function of the volume fraction and the shear rate, $\eta_{\mathrm{mix}} = \eta(\phi, |\dot{\boldsymbol{\gamma}}|)$. ($\eta(0, .) > 0$ is chosen larger than the viscosity of pure fluid to avoid excessively small length scales.

The interaction between the particles is described by the solids pressure p_s.

3.2. Solids pressure

For a volume fraction ϕ higher than the so-called gel forming fraction, ϕ_g, a strongly flocculated suspension forms a network of flocs where the particles are in contact. The network can support normal stresses and resists compression until the force exceeds a volume fraction dependent yield pressure. Then, there will be an irreversible compression of the network resulting in fluid release and increased concentration of solid particles. The irreversibility means in this case that when the external compression load decreases, the suspension will remain compressed. The irreversibility effects are modeled following the method introduced by Yström [10].

A memory function $\phi^*(\boldsymbol{x}, t)$ describes the maximal ϕ encountered since $t = 0$ by a material particle,

$$\phi^*(\boldsymbol{x}, t) = \max_{0\le\tau\le t} \phi(\boldsymbol{x}(\tau), \tau).$$

It satisfies the differential equation

$$\frac{\mathrm{D}\phi^*}{\mathrm{D}t} = \begin{cases} \dfrac{\mathrm{D}\phi}{\mathrm{D}t} & \text{when } \phi \geq \phi^*,\ \dfrac{\mathrm{D}\phi}{\mathrm{D}t} > 0, \\ 0 & \text{otherwise.} \end{cases} \tag{6}$$

and the solids pressure, p_s is a function of ϕ and ϕ^* as

$$p_s(\phi, \phi^*) = \begin{cases} 0 & \text{if } \phi < \phi^*, \\ p_{s,\text{yield}}(\phi) & \text{if } \phi = \phi^*, \end{cases} \tag{7}$$

3.3. Inter-phase momentum transfer

The inter-phase momentum transfer term takes into account the relative motion between the particles and the fluid. According to Anderson and Jackson [11] and Auzerais *et al.* [7],

$$\boldsymbol{m} = \frac{1-\phi}{D(\phi)}(\boldsymbol{v} - \boldsymbol{u}), \tag{8}$$

where we have neglected the virtual mass force term since we only consider slow flows driven by gravity, see also Section 4.

We define $D(\phi) = k(\phi)/\mu$ as the Darcy function, where $k(\phi)$ is the permeability and μ is the viscosity of the fluid.

4. A reduced model

A dimensional analysis is performed to be able to estimate the order of magnitude of the different terms in in Equations (1)–(4). Non-dimensional quantities for a flow in a $H \times H$ box under **g** gravity are introduced as

$$x^* = x/H, \quad y^* = y/H, \quad t^* = t/T, \quad \mathbf{u}^* = \mathbf{u}/U, \quad \mathbf{v}^* = \mathbf{v}/U,$$
$$p^* = p/P, \quad \rho^* = \rho/\Delta\rho, \quad \Delta\rho = \rho_s - \rho_f, \quad \mathbf{e}^* g = \mathbf{g}/G.$$

A characteristic time scale is given by $T = H/U$ where U is the free settling velocity of an individual floc at concentration ϕ_0. U is related to the permeability of the material as $U = \Delta\rho G D_0$ where $D_0 = k(\phi_0)/\mu$. Since the consolidation process is dominated by gravity, the pressure should balance the gravitational forces, $P = \Delta\rho G H$.

Equation (3) together with (5) and (8) can now be written in dimensionless form (the superscript * is dropped for simplicity)

$$F\rho_s\phi\frac{\mathrm{D}\mathbf{u}}{\mathrm{D}t} + \phi\nabla p - \frac{1}{\mathrm{Pe}_s}\nabla\cdot(\phi\boldsymbol{\tau}_s) = -\frac{1}{\mathrm{Pe}}\nabla(p_s) + \rho_s\phi\mathbf{e}_g + \frac{1-\phi}{D(\phi)}(\mathbf{v}-\mathbf{u}), \tag{9}$$

where the dimensionless numbers, Pe, Pe_s and the Froude number, F, are defined as

$$\mathrm{Pe} = \frac{G\Delta\rho H}{P_{s0}}, \quad \mathrm{Pe}_s = \frac{G\Delta\rho H}{\tau^0}, \quad F = \frac{U^2}{GH}$$

with $\tau_0 = U\eta_0/H$. The stress scale factors are $\eta_0 = \eta(\phi_0, u_{\text{wall}}/H)$ and $P_{s0} = p_s(\phi_0)$ where u_{wall}/H is a measure of the shear rate. Equation (4) can be treated in similar way using the same dimensionless groups with the Froude number appearing in front of the inertial terms.

Since the suspension is dense, the permeability will become extremely small in areas where the concentration of particles is high. In these regions the sedimentation velocity will be low and F will be small, typically of order 10^{-9}, compared to $1/\mathrm{Pe}$ and $1/\mathrm{Pe}_s$ which are of order 10^{-5}, for full details see [16]. Therefore, all terms of $\mathcal{O}(F)$ will be discarded from the equations. As a consequence, the fluid velocity field can be eliminated and the following coupled hyperbolic-elliptic system is obtained for the unknowns ϕ, p and $\boldsymbol{u}$, again in dimensional form,

$$\phi_t + \nabla \cdot (\phi \boldsymbol{u}) = 0, \tag{10}$$

$$\nabla \cdot (\boldsymbol{u} - \tilde{D}\nabla p) = 0, \tag{11}$$

$$\nabla p - \nabla \cdot (\eta(\nabla \boldsymbol{u} + \nabla \boldsymbol{u}^T - \tfrac{2}{3}\nabla \cdot \boldsymbol{u})) = -\nabla(p_s) + \phi(\rho_s - \rho_f)G\boldsymbol{e}_g. \tag{12}$$

Here $\boldsymbol{u} = (u, v)$ and u and v are the particle velocity field components in the x- and y-directions and $p = p_f - p_0 - p_f \boldsymbol{e}_g \cdot \boldsymbol{x}$ is the reduced pressure, sometimes called the excess pore pressure. The Darcy coefficient $\tilde{D} = (1-\phi)D(\phi)$, the effective solids pressure $p_s = p_s(\phi, \phi^*)$, and the mixture viscosity $\eta = \eta(\phi|\dot{\gamma}|)$ are determined by experimental data and will be defined in Section 6.

5. 1D model

The 1D consolidation model is the base for the parameter fitting to experimental data. In the measurements there is no unloading and $\phi^* = \phi$ and $\phi_g = \phi_0$, the initial concentration. Let $y \in [0, H]$ where H is the height of the container. With the gravitational force acting in the negative y-direction (see Figure 1), the system of Equations (10)–(12) is reduced to

$$\frac{\partial \phi}{\partial t} + \frac{\partial}{\partial y}(\phi v) = 0, \tag{13}$$

$$\frac{\partial}{\partial y}(\tilde{D}\frac{\partial p}{\partial y}) - \frac{\partial v}{\partial y} = 0, \tag{14}$$

$$\frac{4}{3}\frac{\partial}{\partial y}(\eta\frac{\partial v}{\partial y}) - \frac{\partial p}{\partial y} = \frac{\partial p_s}{\partial y} + F\phi, \tag{15}$$

where $\tilde{D} = D(\phi)(1-\phi)$, $\eta = \eta(\phi)$, $p_s = p_s(\phi)$ and we have introduced $F = g\Delta\rho = g(\rho_s - \rho_f)$. The boundary conditions are that $v = 0$ and $\partial p/\partial y = 0$ at $y = 0$ and $y = H$.

Equation (14) can be integrated using the boundary condition at $y = 0$ and together with Equation (15) yields a differential equation for v,

$$\frac{4}{3}\frac{\partial}{\partial y}\left(\eta\frac{\partial v}{\partial y}\right) - \frac{v}{\tilde{D}} = \frac{\partial p_s}{\partial y} + \phi F. \tag{16}$$

In many applications the viscous term can be neglected depending on the size of a length scale determined by the viscosity and the permeability, as seen from the following discussion.

Assume that ϕ is bounded but can be discontinuous and that $p_s(\phi(.,t)) \in H^1[0, H]$. Then, if there exists a smooth solution v the following estimate can be obtained by multiplying Equation (16) with v, integrating by parts and using the Poincaré inequality:

$$\|v\| \leq \frac{F\|\phi\| + \|(p_s)_y\|}{\dfrac{1}{|\tilde{D}|_\infty} + \dfrac{4}{3}\dfrac{\pi^2}{H^2}\eta_{\min}}, \tag{17}$$

where

$$\eta_{\min} = \min_{0\leq y\leq H} \eta(y).$$

Here $\|\cdot\|$ is the usual L_2 norm defined by

$$\|f\|^2 = (f, f) = \int_0^H |f|^2 \, \mathrm{d}y. \tag{18}$$

The particle velocity, v, is directly related to the time scale of the consolidation process. In this case it is the product of permeability and viscosity that is important for the time scale. If $\tilde{D}(\phi)\eta/H^2$ is small, the time scale is determined by the permeability related Darcy function, $\tilde{D}(\phi)$. However, if $\tilde{D}(\phi)\eta/H^2$ becomes large, the viscosity will influence the sedimentation speed and time scale of the process.

In many practical cases $\tilde{D}\eta/H^2 \ll 1$. The velocity profile shows a boundary layer at $y = 0$ and for $y \gg \sqrt{\tilde{D}\eta}$ the viscous term can be neglected, and

$$v = -\tilde{D}((p_s)_y + \phi F). \tag{19}$$

With v according to (19), (13) becomes a convection-diffusion equation for ϕ

$$\phi_t - F(\tilde{D}\phi^2)_y = (\phi\tilde{D}(p_s)_y)_y. \tag{20}$$

Equation (20) is referred to as the classical 1D model. It is used in many applications and treated from both mathematical and numerical points of view in for example [7], [8], and [9].

6. Parameter fitting

This work is concerned with the consolidation of sludges from industrial waste streams, sometimes with organic content. The application requires that the material data needed should be furnished by techniques which can be applied routinely. The constitutive models used for our numerical experiments are fitted to experimental data supplied by Alfa Laval Separation using filter press devices and torque vane rheometers. An application to mineral suspensions is treated in depth in Green [12].

Usually the experimental apparatus is limited to a certain range of the parameters. In particular, the industrial sludge studied in this work has very low permeability and standard filter press devices require long times to reach equilibrium. This is acceptable for research but for routine applications other devices must be developed.

A fundamental problem is the determination of the solids volume fraction. This is easy for mineral suspensions where the density of the solids is accurately known, but we have not found any experimental technique which can measure this quantity for organic sludge. Solids weight fraction, however, is easily determined by drying, and it has been necessary to convert this to solids volume fraction by assumptions on intra-cellular water content.

The yield stress is well determined; all the experimental data is fitted to within a factor two by the power law below, see Equation (21). The permeability is much more uncertain,

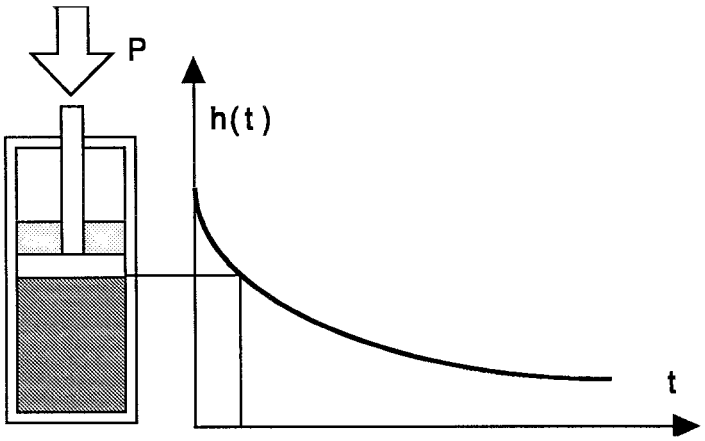

Figure 2. Filter press device. Walls are impermeable, the piston is porous and the expelled fluid (shown in light gray) is drained from the top. Position is recorded as function of time after application of a load step P.

for several reasons. The test batches show larger systematic variations, and some tests were disturbed by gas development. The gas influences the initial consolidation more than it does the final 'steady state'. Permeability also varies with concentration much more than yield stress, see Figure 3 and Equation (23).

The rheological measurements required handling and 're-constitution' of the sludge samples which may have influenced the interpretations. It was found in the simulations that lower shear rates occur than were covered in the measurements. This 'extrapolation' is also a source of uncertainty.

6.1. Filter press determination of yield stress

The filter press device is shown in Figure 2. The load P is increased in steps and the resulting movement recorded until steady state is reached. Gravity can be neglected, so at steady state the concentration is uniform, and yield pressure is equal to the applied load. Concentration is calculated from the initial concentration and piston position. Several sets of data were used and gave quite consistent fits to a power law,

$$p_{s,\text{yield}}(\phi) = C_{ps}\phi^{4{\cdot}846} \tag{21}$$

where $C_{ps} = 5 \times 10^6$ Pa and $\phi > \phi_g$.

6.2. Filter press determination of permeability

Assuming an initial uniform concentration and small load increments we may reduce the model to a diffusion equation with a constant diffusivity, with a step change in concentration at one end. The exact solution is of similarity type $f(y/\sqrt{t})$ and it follows that the position for small t follows a $\sqrt{t}$-curve. Permeability can be read off from the initial slope of h *vs.* $\sqrt{t}$. Indeed, one has

$$\frac{k}{\mu} = \frac{\pi}{4m\phi}\left(\frac{\left.\dfrac{\mathrm{d}h}{\mathrm{d}\sqrt{t}}\right|_{t=0}}{\dfrac{h(0)}{h(\infty)} - 1}\right)^2, \tag{22}$$

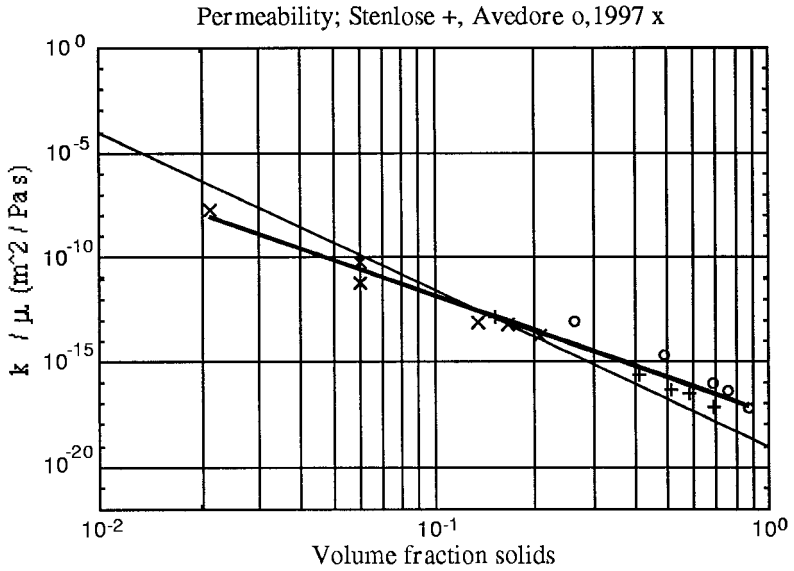

Figure 3. Permeability as function of volume fraction solids. Data for three sludges shown, '1997' *o* and *x*, '1992' +. The thick line is a least-squares fit using all the data, the thin line only *x* and +.

where k/μ is the Darcy function $D(\phi)$ and m the compression module $\mathrm{d}p_{s,\mathrm{yield}}/\mathrm{d}\phi$. Thus, determination of the permeability k requires estimation of initial slope, long-term limit, and differentiation of $p_{s,\mathrm{yield}}$. The results for some of the data are summarized below and in Figure 3. The volume fraction solids changes about a factor four in an experiment such as the one shown in Figure 4 where permeability changes by three to four decades.

$$D(\phi) = C_D \phi^{-7{\cdot}41}, \tag{23}$$

where $C_D = 4{\cdot}6 \times 10^{-18}$ m^2 Pa^{-1} s^{-1}. Note the strong variation with ϕ. The model has to be modified in the limit $\phi \to 0$ to give finite velocities; this is done. by extrapolating to $\phi = 0$ along the tangent at $\phi = 0{\cdot}05$. The modification has to be done in such a way that the sharp clear fluid-suspension interface observed in practice is kept. Figure 4 shows an experiment with five successive load increases on the same sample, plotted lexicographically. The sample in the process is compressed from 8 mm to 2·1 mm in the course of about five days. The simulation reproduces the measured consolidation well with the exception of the two last load steps. The drops at $t = 0$, very small in the first load steps and increasing with time, indicate gas formation from fermentation, which has not been modeled. The parameters used were obtained by fitting to all experiments, not only the one shown here. There is almost straight line dependence of h on $\sqrt{t}$ for small t.

6.3. Shear thinning viscosity

Flocculated suspensions are known to be shear thinning, see Barnes *et al.* [13, Chapter 7]. This is validated by experimental shear force data given as a function of volume fraction, ϕ and shear rate, $|\dot{\boldsymbol{\gamma}}|$. These data are fitted to a generalized non-Newtonian viscosity law, see Bird *et al.* [14, pp. 171–175]. This model for shear-thinning is combined with a volume fraction dependence yielding:

$$\eta_{\mathrm{mix}} = \eta(\phi, |\dot{\boldsymbol{\gamma}}|) = C_\eta \phi^{3{\cdot}4} \left(1 + \frac{|\dot{\boldsymbol{\gamma}}|}{0{\cdot}05}\right)^n, \tag{24}$$

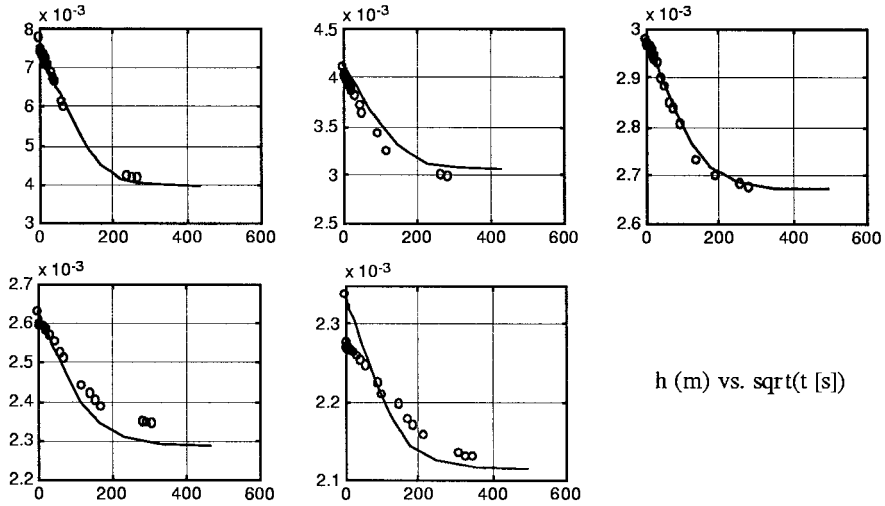

Figure 4. Filter press experiment and simulation. o: measurement, solid line: simulation.

where $C_\eta = 9{\cdot}15 \times 10^7$ Pas and $n = -0{\cdot}9$. The shear rate is defined as

$$\dot{\boldsymbol{\gamma}} = \nabla \boldsymbol{u} + \nabla \boldsymbol{u}^T, \quad |\dot{\boldsymbol{\gamma}}| = \sqrt{\tfrac{1}{2}|(tr\dot{\boldsymbol{\gamma}})^2 - tr(\dot{\boldsymbol{\gamma}} \cdot \dot{\boldsymbol{\gamma}})|}.$$
$$tr\dot{\boldsymbol{\gamma}} = \sum_n (\dot{\boldsymbol{\gamma}})_{nn}. \tag{25}$$

7. Numerical treatment of the 2D model

The setup for the 2D test case is a closed container of size $H \times H$ with a moving bottom wall to induce shear on the suspension in addition to the influence of gravity, see Figure 1. This test problem can be described by Equations (10)–(12) with suitable boundary conditions for the velocity components and the pressure. On all boundaries, wall normal velocity component vanishes as does the reduced pressure normal derivative. It follows that there is no fluid flow through the walls. We assume that the friction between the bottom wall and the particle phase is large and a no-slip condition is imposed there: $u = u_{\text{wall}}(x)$. On the side walls and on the top we assume perfect slip, *i.e.* vanishing wall shear stress. This models a device with different materials in side and bottom walls. It was chosen to let the sediment easily slide up the wall it meets.

The initial conditions for ϕ and ϕ^* are given by: $\phi(x, y, 0) = \phi_0(x, y)$ and $\phi^*(x, y, 0) = \phi_0$. To characterize the suspension we use the material models defined in Section 6 and we assume that the models and parameters determined by 1D devices are also valid in the 2D case.

The elliptic-hyperbolic system is solved in the following fashion. With ϕ and ϕ^* known at, say, t, the elliptic system (11)–(12) is solved for velocities $\boldsymbol{u}$ (and p) with coefficients and source functions computed from $\phi(t)$ and $\phi^*(t).\phi$ and ϕ^* at $t + \Delta t$ are then computed by the scheme below. The elliptic system of equations is discretized in space by central finite differences of second order. This choice of discretization is subject to step size restriction given by

$$(\Delta x, \Delta y) \leq \sqrt{\eta \tilde{D}} \tag{26}$$

in order to avoid oscillative solutions, *cf.* the mesh Péclet number restriction for convection-diffusion problems, see Morton [15, Chapter 7]. To use a uniform grid that satisfies Equation (26) is too costly. Therefore a priori fixed mesh grading is used with more grid points close to the bottom of the container where the minimum value of $\tilde{D}$ occurs. In computational cells where the step size restriction is not fulfilled, the permeability is artificially increased in order to stabilize the scheme.

Since the model contains only pressure gradients, the pressure will be uniquely determined only up to an additive constant. In order to fix a unique solution we solve the elliptic problem as a constrained minimization problem, see Gustavsson [16].

The resulting linear system of equations is ill-conditioned due to the variation of permeability and viscosity. After diagonal scaling it is solved by Gaussian elimination taking advantage of the sparsity of the matrix. The matrix factorization is currently the most time-consuming part of the simulation.

The hyperbolic Equation (10) is strongly non-linear and requires a conservative upwind method. Simple one-sided differences are inappropriate because the sign of the characteristic speed will change during the computation. Instead ideas from Godunov's method, described in *e.g.* Le Veque [17, pp. 136–157], are used.

Equation (10) can be written as

$$\phi_t + g(\phi, u(x, y; \phi))_x + f(\phi, v(x, y; \phi))_y = 0 \tag{27}$$

to identify the flux functions $g = \phi u(x, y; \phi)$ and $f = \phi v(x, y; \phi)$. The velocity components u and v are obtained as the solution to the elliptic system of equations, (11) and (12). The numerical flux functions used in the scheme require the characteristic speeds $g_\phi = u + \phi u_\phi$ and $f_\phi = v + \phi v_\phi$. Since f and g do not depend only on local values of ϕ, the difference formula is chosen from numerical approximations to u_ϕ and v_ϕ, see Gustavsson [16]. The scheme thus becomes equivalent to the Godunov scheme in the limit of vanishing viscosity.

The linear advection equation for ϕ^*, Equation (6), is solved by a first-order upwind scheme where the differences are chosen depending on the characteristic velocities, the components of the particle velocity field. The time step Δt is chosen such that the Godunov scheme and the linear upwind scheme fulfill the CFL-condition.

8. Results and discussion

The influence of shear on the consolidation process is of great interest. Physical experiments and interpretations of belt filter press operations show increased consolidation speed as a result of applied shear. This phenomenon is not reproduced by this model, see Gustavsson and Oppelstrup [18]. Closely related to the shear forces is the viscosity of the suspension. For this reason we study the effect of different viscosity models on the process.

In Section 5 we saw that the size of the viscosity influenced the time scale of the 1D process. To investigate if this holds also in the 2D test case we use a viscosity model that only depends on the volume fraction.

$$\eta(\phi) = C\eta_0\phi^{3{\cdot}4}. \tag{28}$$

Simulations are performed with $\eta_0 = 9{\cdot}15 \times 10^7$ Pas where $C = 0{\cdot}1$, 1 and 10 to obtain different sizes of the 'over-all-viscosity'.

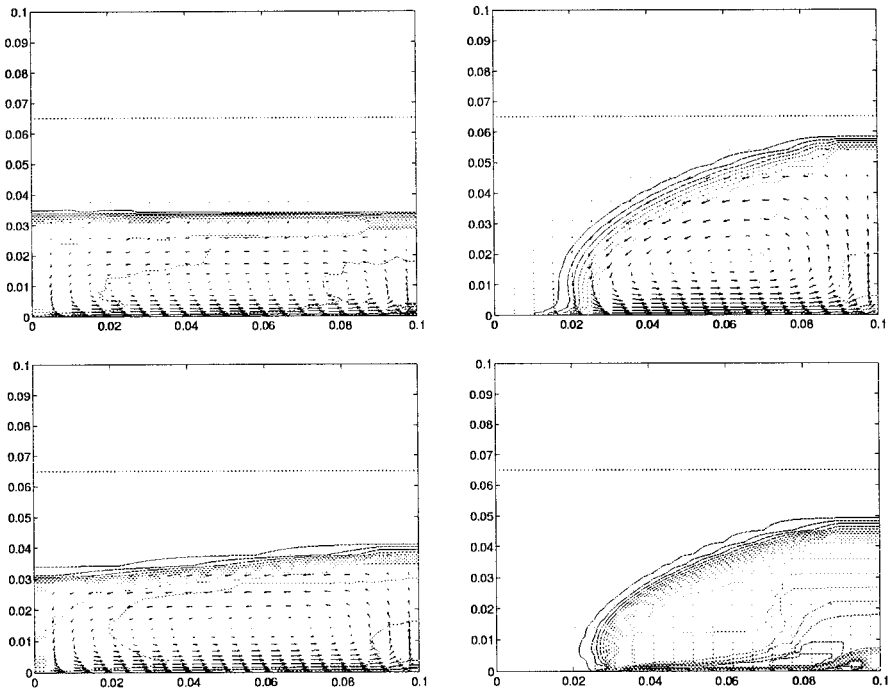

Figure 5. Concentration contours at time $t = 250$ s. The computations are performed with different viscosity models. The upper left, right and lower left figures present the results of the non-shear thinning model (28) with $\eta_0 = 0{\cdot}1$, 1 and 10. In the lower right figure the shear thinning model (24) is used. $G = 10\,000$ ms^{-2} and $u_{\text{wall}} = 0{\cdot}01$ ms^{-1}. The dotted line indicates the initial condition.

The results displayed in Figure 5 show that the size of the viscosity is important also in the 2D case. As the viscosity becomes larger the suspension tends to behave more like a solid and 'climbs up' the right wall. Also, the boundary layer grows with increasing viscosity. This slows down the consolidation process and a lower mean concentration is obtained, see Figure 6.

We define the mean concentration in the dense part of the suspension as

$$\bar{\phi} = \frac{1}{A_c} \int_{A_c} \phi \, \mathrm{d}A_c, \tag{29}$$

where A_c is the area for which ϕ is larger than a chosen threshold value, ϕ_c. In this case $\phi_c = 0{\cdot}05$.

Next, we use a shear thinning viscosity model, (24). In Figure 6 we note that this model yields a higher mean value of ϕ, even though the 'over-all-viscosity' is of the same order as with $\eta = 10$ in the first computation. One effect of shear thinning is smaller effective viscosity close to the bottom due to high shear rates. Note also in the lower right plot in Figure 5 that the suspension starts to slip close to the bottom wall and a thin fluid layer is observed.

In all the computations the following parameters were used:

- $H = 0{\cdot}1$ m,
- $G = 10\,000$ ms^{-2},

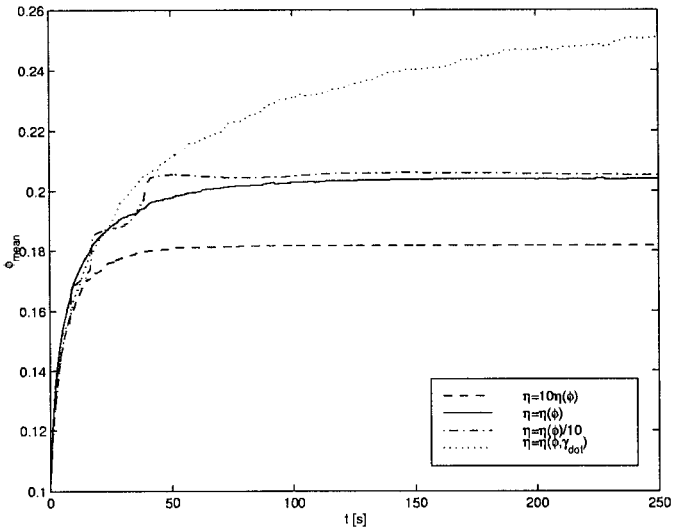

Figure 6. The mean concentration as a function of time for different viscosity models. $G = 10000$ ms^{-2} and $u_{\text{wall}} = 0{\cdot}01$ ms^{-1}. Dotted line: viscosity is a function of the shear rate ana concentration.

- $\Delta\rho = 1000$ kgm^{-3},
- Number of grid points $N_x = N_y = 40$.

9. Conclusions and future work

A numerical model for consolidation of dense suspensions was developed and constitutive relations fitted to measurements. The simulations of 1D cases show results in good agreement with observations and with expectations.

For 2D cases, simulation results are plausible. Quantitative experimental 2D studies are necessary to validate and further develop the model but are so far lacking.

Currently, the expected effects of shear on the process are not well reproduced. Several remedies have been suggested. The material should resist shear also in equilibrium. The plastic material models used for geo-mechanics are interesting. The shape of the plastic yield surface for such materials make shear forces decrease the normal forces necessary for compression, and shear will speed up consolidation by that effect. It has also been suggested that permeability should depend on the history of a material particle and be greater for a particle in dilation than compression at the same ϕ, Eiken [19]. Recent numerical experiments have shown that such a model does give the expected result. This is an ongoing study and in its current form, it is overly sensitive to a parameter which defines the floc size of the material in dilation, and for the value of which we have no good theoretical guidelines.

The sensitivity of the results to the viscosity model also suggests that a more detailed study needs to be performed to fully understand the effects of shear and viscosity. Direct numerical simulations of fluid-particle suspensions can be a helpful tool in order to study these effects on the particle scale.

For 2D models, the grid resolution is currently a limiting factor for numerical experiments. Iterative solution of the elliptic system offers memory economy but we have so far not found an effective pre-conditioner.

Acknowledgements

The project was supported by NUTEK and Alfa Laval Separation AB through the Parallel Scientific Computing Institute. Jon Eiken and Bent Madsen of Alfa Laval Separation AB have supplied the experimental data and invaluable engineering, process, and modeling experience which is gratefully acknowledged.

References

1. R. Glowinski, T.-W. Pan, T.I. Hesla and D.D. Joseph, A distributed Lagrange multiplier/fictitious domain method for particulate flows. *Int. J. Multiphase Flow* 25 (1999) 755–704.
2. B. Maury, Direct simulations of 2D fluid-particle flow in biperiodic domains. *J. Comp. Phys.* 156 (1999) 325 –351.
3. D.A. Drew and S.L. Passman, *Theory of Multicomponent Fluids*. Applied Mathematical Science, vol. 135. Berlin: Springer (1999) 308 pp.
4. M.C. Bustos and F. Concha and R. Bürger and E.M. Tory, *Sedimentation and Thickening, Phenomenological Foundation and Mathematical Theory*. Dordrecht: Kluwer Academic Publisher (1999) 285 pp.
5. S. Zahrai, *On The Fluid Mechanics of Twin- Wire Formers*. PhD thesis, Dept. of Mechanics, Royal Institute of Technology, Sweden (1997) 84 pp.
6. H. Enwald and E. Peirano and A-E. Almstedt, Eulerian two-phase flow theory applied to fluidization. *Int. J. Multiphase Flow* 22 (1996) 21–46.
7. F.M. Auzerais and R.J. Jackson and W.B. Russel, The resolution of shocks and the effect of compressible sediments in transient settling. *J. Fluid Mech.* 195 (1988) 437–462.
8. R. Bürger and F. Concha, Mathematical model and numerical simulation on the settling of flocculated suspensions. *Int. J. Multiphase Flow* 24 (1998) 1005–1023.
9. M. Dorobantu, *One-Dimensional Consolidation Models*. Licentiate's thesis, Dept. of Numerical Analysis and Computing Science, Royal Institute of Technology, Sweden (1997) 54 pp.
10. J. Yström, *On the Numerical Modeling of Concentrated Suspensions and of Viscoelastic Fluids*. PhD thesis, Dept. of Numerical Analysis and Computing Science, Royal Institute of Technology, Sweden (1996) 150 pp.
11. T.B. Anderson and R. Jackson, Fluid mechanical description of fluidized beds *Industrial and Engineering Chemistry Fundamentals* 6 (1967) 527–538.
12. M.D. Green, *Characterisation of Suspensions in Settling and Compression*. PhD Thesis, Dept. of Chemical Engineering, University of Melbourne, Australia (1997) 246 pp.
13. H.A. Barnes and J.F. Hutton and K. Walters, *An Introduction to Rheology*. Amsterdam: Elsevier Science Publisher (1989) 199 pp.
14. R.B. Bird and C.F. Curtiss and R.C. Armstrong and O. Hassager, *Dynamics of Polymeric Liquids*. New York: Wiley Interscience (1987) 649 pp.
15. K.W. Morton, *Numerical Solution of Convection-Diffusion Problems*. London: Chapman & Hall (1996) 372 pp.
16. K. Gustavsson, *Simulation of Consolidation Processes by Eulerian Two-Fluid Models*. Licentiate's thesis, Dept. of Numerical Analysis and Computer Science, Royal Institute of Technology, Sweden (1999) 60 pp.
17. R.J. LeVeque, *Numerical Methods for Conservations Laws*. Basel: Birkhäuser Verlag (1992) 214 pp.
18. K. Gustavsson and J. Oppelstrup, *A Numerical Study of the Consolidation Process of Flocculated Suspensions Using a Two-Fluid Model*. Proceedings, The Third European Conference on Numerical Mathematics and Advanced Applications (ENUMATH), World Scientific (1999)
19. J. Eiken, Private Communication.